Optik 125 (2014) 5002–5006

Contents lists available at ScienceDirect

Optik

journal homepage: www.elsevier.de/ijleo

Multi-focus image fusion based on robust principal component analysis and pulse-coupled neural network

Yongxin Zhang[a,b], Li Chen[a,*], Zhihua Zhao[a], Jian Jia[c], Jie Liu[d]

[a] School of Information Science and Technology, Northwest University, Xi'an 710127, China
[b] Luoyang Normal University, Luoyang 471022, China
[c] Department of Mathematics, Luoyang Normal University, Luoyang 471022, China
[d] School of Mathematics and Computer Science, Shaanxi University of Technology, Hanzhong 723000, China

ARTICLE INFO

Article history:
Received 9 August 2013
Accepted 10 April 2014

Keywords:
Image fusion
Robust principal component analysis
Pulse-coupled neural network
Firing times

ABSTRACT

Multi-focus image fusion combines multiple source images with different focus points into one image, so that the resulting image appears all in-focus. In order to improve the accuracy of focused region detection and fusion quality, a novel multi-focus image fusion scheme based on robust principal component analysis (RPCA) and pulse-coupled neural network (PCNN) is proposed. In this method, registered source images are decomposed into principal component matrices and sparse matrices with RPCA decomposition. The local sparse features computed from the sparse matrix construct a composite feature space to represent the important information from the source images, which become inputs to PCNN to motivate the PCNN neurons. The focused regions of the source images are detected by the firing maps of PCNN and are integrated to construct the final, fused image. Experimental results demonstrate that the superiority of the proposed scheme over existing methods and highlight the expediency and suitability of the proposed method.

1. Introduction

Multi-focus image fusion is a process in which images with different settings are integrated to produce a new image that contains all relevant objects in focus, which is useful for human or machine perception [1]. Image fusion schemes can be categorized into two groups: spatial domain fusion and transform domain fusion [2]. The spatial domain fusion methods [3–5] are easy to implement and have low computational complexity, but they may produce blocking artifacts and compromise the fusion quality. In contrast, transform domain fusion methods [6–8] may achieve improved contrast and better signal-to-noise ratio [9] than spatial domain fusion methods.

The pulse-coupled neural network (PCNN) is a novel visual cortex-inspired neural network characterized by the global coupling and pulse synchronization of neurons [10–12]. In image fusion, the PCNN is a single layered, two-dimensional, laterally connected neural network of pulse-coupled neurons, which are connected with image pixels each other [13]. Many multi-focus image fusion methods based on PCNN have been proposed [14–17]. However, these methods are time consuming (parameters are most adjusted manually) and ignore noise (noise may affect the accuracy of focused regions detection and compromise the fusion quality).

In order to avoid the problems mentioned above, a new method based on robust principal component analysis (RPCA) and PCNN is proposed. RPCA is an effective way to construct low-dimensional linear-subspace representations from high-dimensional data such as images [18]. RPCA decomposes an image into a low-rank matrix which corresponds to the background and a sparse one which represents important image features [19]. T. Wan et al. [20] have investigated its potential application in multi-focus image fusion and have achieved consistently good fusion results, but their method requires longer computational time than traditional methods. In this paper, RPCA is employed to capture the features of objects in source images and the local features of the sparse matrix are computed to motivate the PCNN neurons. The sparse matrix is computed through an in-exact augmented Lagrange multiplier (IALM) method [21,22], a fast version of implementation for recovering low-rank matrices. RPCA can improve the robustness of fusion and the precision of selection of in-focus objects. The biological characteristics of PCNN can take full advantage of the local features computed from sparse matrices and improve the accuracy of the determination of in-focus objects. The proposed method is robust to noise interference and suitable to different fusion tasks.

* Corresponding author. Tel.: +86 18637930027.
E-mail addresses: chenli@nwu.edu.cn, tabo126@126.com (L. Chen), jiajian@nwu.edu.cn (J. Jia), slg_liujie@126.com (J. Liu).

http://dx.doi.org/10.1016/j.ijleo.2014.04.002
0030-4026/

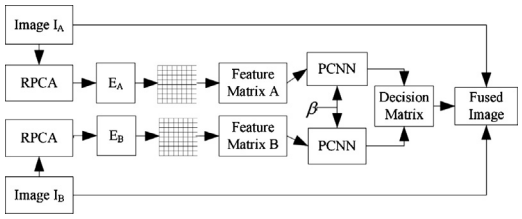

Fig. 1. Block diagram of proposed multi-focus images fusion framework.

The rest of the paper is organized as follows. In Section 2, the new method based on RPCA and PCNN for image fusion will be described in detail. In Section 3, extensive simulations are performed to evaluate the performance of the proposed method. In addition, several experimental results are presented and discussed. Finally, concluding remarks are made in Section 4.

2. Multi-focus image fusion based on RPCA and PCNN

In this section, a novel method for multi-focus image fusion is proposed. The proposed fusion framework is depicted in Fig. 1. For simplicity, this paper assumes that there are only two source images, namely I_A and I_B, the proposed method may be used for fusion of more than two source images, which are assumed to be pre-registered. Image registration is not included in this framework. The proposed fusion method consists of the following five steps: vectorization of source images, vector decomposition, block division and feature map construction, construction of decision matrix, and image fusion.

2.1. Vectorization of source images

As mentioned above, the data matrix D represents the source image after vectorization. However, the time for completing RPCA decomposition is affected by the vector form of input data matrix D. In order to select the optimal vector form of this matrix, we compare rates of RPCA decomposition on different vector forms. The total running time includes both the time consuming step of RPCA decomposition and vector conversion before and after RPCA decomposition. For comparison, the multi-focus images are converted to corresponding forms of input matrix before RPCA decomposition. The sparse matrix of RPCA decomposition is converted to a matrix corresponding to the source image after RPCA decomposition.

Table 1 lists the running times for RPCA decomposition performed on three different forms of several multi-focus images. It can be seen that the running time for the form of $D = I,\ I \in \mathbb{R}^{MN\times 1}$ is shortest for all images analyzed. The running time for the form of $D = [I_A I_B],\ I_A,\ I_B \in \mathbb{R}^{MN\times 1}$ is shorter than that of $D = I,\ I \in \mathbb{R}^{M\times N}$. The multi-focus images analyzed are 'Clock' (size 512×512), 'Pepsi' (size 512×512), 'Lab' (size 640×480), 'Disk' (size 640×480), 'Rose' (size 512×384) and 'Brain' (size 256×256).

The source images $\{I_A, I_B\},\ I_A,\ I_B \in \mathbb{R}^{M\times N}$ are converted into column vectors $I_A, I_B \in \mathbb{R}^{MN\times 1}$, respectively, before RPCA decomposition. Column vectors $I_A, I_B \in \mathbb{R}^{MN\times 1}$ are decomposed into principal matrices $A_A, A_B \in \mathbb{R}^{MN\times 1}$ and sparse matrices $E_A, E_B \in \mathbb{R}^{MN\times 1}$ by RPCA, respectively. The sparse matrices $E_A, E_B \in \mathbb{R}^{MN\times 1}$ are computed through the inexact augmented Lagrange multipliers algorithm (IALM) of RPCA [22], which has been reported to yield similar results to other low rank matrix recovery methods with much less consumption. The sparse matrices $E_A, E_B \in \mathbb{R}^{MN\times 1}$ are then converted into matrices $E_A, E_B \in \mathbb{R}^{M\times N}$ corresponding to source images I_A and I_B, respectively. Thus, D is given by:

$$D = I, \quad I \in \mathbb{R}^{MN\times 1} \tag{1}$$

where $D \in \mathbb{R}^{MN\times 1}$ is the input matrix for the RPCA model. D_A and D_B ($D_A, D_B \in \mathbb{R}^{MN\times 1}$) are the source images after vectorization.

Table 1
Comparison of the running time for RPCA decomposition of multi-focus images.

Multi-focus images	Vector format		
	$D = I,\ I \in \mathbb{R}^{M\times N}$	$D = I,\ I \in \mathbb{R}^{MN\times 1}$	$D = [I_A I_B],\ I_A,\ I_B \in \mathbb{R}^{MN\times 1}$
Clock	10.2310	0.3794	1.0003
Pepsi	9.7374	0.3884	1.0153
Lab	21.0188	0.4562	1.1663
Disk	17.3640	0.4460	1.1848
Rose	8.0979	0.3143	0.7859
Brain	2.4941	0.1329	0.2775

2.2. Vector decomposition based on RPCA

RPCA decomposition is performed on vector D to obtain a principal matrix $A \in \mathbb{R}^{MN\times 1}$ and a sparse matrix $E \in \mathbb{R}^{MN\times 1}$. The sparse matrix E is computed by IALM and then converted into a $M \times N$ matrix. Thus, E_A and E_B ($E_A, E_B \in \mathbb{R}^{M\times N}$) corresponding to the source images can be obtained.

2.3. Block division and feature maps construction

Sparse matrices E_A and E_B are next decomposed into blocks. Let $E_A^{(k)}$ and $E_B^{(k)}$ denote the kth block of sparse matrices E_A and E_B, respectively. The EOL of each matrix block can be calculated as follows [23]:

$$\mathrm{EOL} = \sum_i \sum_j (E_{ii}^2 + E_{jj}^2) \tag{2}$$

$$\begin{aligned} E_{ii} + E_{jj} = {} & -E(i-1,j-1) - 4E(i-1,j) - E(i-1,j+1) \\ & - 4E(i,j-1) + 20E(i,j) - 4E(i,j+1) - E(i+1,j-1) \\ & -4E(i+1,j) - E(i+1,j+1) \end{aligned} \tag{3}$$

where $E(i,j)$ indicates the value of the element at the position (i,j) in the sparse matrix block. Let $\mathrm{EOL}_{(k)}^{E_A}$ and $\mathrm{EOL}_{(k)}^{E_B}$ be the EOL of $E_A^{(k)}$ and $E_B^{(k)}$, respectively. The EOL of corresponding blocks of the two sparse matrices constructed the feature maps F_A and F_B, respectively.

2.4. Construction of decision matrix based on PCNN

F_A and F_B become the input to PCNN to motivate the neurons and generate neuron pulses. Let $T_A(k)$ and $T_B(k)$ denote the firing time of the kth feature element in feature maps F_A and F_B, respectively. Thus, a decision matrix $H \in \mathbb{R}^{M\times N}$ can be constructed for recording the comparison results according to the selection rule as follows:

$$H(i,j) = \begin{cases} 1 & T_A(k) \geq T_B(k) \\ 0 & \text{otherwise} \end{cases} \tag{4}$$

where "1" in H indicates that the pixel (i,j) of the kth block of image I_A is in focus while "0" in H indicates that the pixel (i,j) of the kth block of image I_B is in focus.

2.5. Image fusion based on decision matrix

However, judging by firing times of the PCNN alone is not sufficient to identify all focused blocks. There are also thin protrusions, narrow breaks, thin gulfs and small holes in H. Morphological operations [24] are performed on H to eliminate the defects in H.